The Cutting Mechanism of Fine-Grain Abrasive Stone

By

Tokio SASAKI and Kenjiro OKAMURA*

The depth of cut for the individual abrasive grains and the cutting resistance affecting the individual cutting points that are produced in honing or superfinishing operations are important factors to investigate the cutting mechanism of fine-grain abrasive stone. But the above factors depend on the number of cutting points on the stone surface which comes in contact with the work surface.

In this paper, the contact mechanism between the stone and the work surface has been investigated theoretically in order to determine the number of cutting points. And the number of cutting points is obtained as a function of the roughness of the stone surface, the pressure on the stone and the hardness of the work material.

Then, for checking the validity of this theory, the mean depth of cut $(t_m)_{th}$ derived from the theoretical investigation of the contact mechanism is compared with the mean depth of cut $(t_m)_{ex}$ which can be obtained from the stock removal per unit time and the number of cutting points on the stone surface in an actual superfinishing operation. As a result of this comparison, the validity of the theoretical equation for the number of cutting points was established by inquiring into the causes of the difference between $(t_m)_{th}$ and $(t_m)_{ex}$ and their influence on the number of cutting points.

Symbols

The following symbols are used in this paper :

A =total true contact area

A_w =apparent contact area

B =bond combining ratio

C_t =cutting depth per unit time

G =grain combining ratio

H =maximum height of asperity or roughness of contact surface of stone

M =number of asperities per unit depth

N =total number of surface units contained within the measured length L

P =porosity of stone

R_H =bond hardness of stone

---

* Department of Mechanical Engineering

S_c = mean cutting sectional area of grain

S_i = contact area of one asperity

T = maximum depth of indentation

W = contact load

a = amplitude of stone

d_g = mean diameter of grain

f = frequency of stone

m = working time

n = number of cutting points on the contact surface of stone, or number of asperities into contact

n_a = number of grains per unit area

p_m = flow pressure of work material

p = stone pressure

$(t_m)_{th}$ = theoretical mean cutting depth of grain

$(t_m)_{ex}$ = experimental mean cutting depth of grains

u = deviation from the median line of profile curve

$\bar{v}$ = mean relative cutting speed of work and stone

v_w = work speed

$f(u)$ = probability density of surface units distribution

Θ = cutting direction angle

Ψ – slope angle of asperity

σ = standard deviation

$\varepsilon\sigma$ = projection width which can be comprised in one surface unit

ρ = specific weight of stone

vol_w = stock removal per unit time

Introduction

In order to investigate the cutting mechanism of fine-grain abrasive stone such as a grinding wheel, it is necessary to find the depth of cut for the individual abrasive grains and the cutting resistance affecting the individual cutting points. Further the number of cutting points on the contact surface of the stone is the fundamental factor for determining their values. In a grinding operation, the number of cutting points can be obtained by counting the number of stamped points which are made by rolling a grinding wheel across a glass plate or a freshly ground surface coated with a layer of soot approximating the mean depth of cut for individual cutting points in thickness[1]. But the above method can not be applied in this case for two reason, the grain size is too small and the value of the cutting depth can not be known.

The number of grains per unit area n_a which intersect the optional plane in the inner parts of 'a stone is defined as follows

$$n_a = \frac{6}{\pi} \frac{G}{d_g^2} \tag{1}$$

where G = grain combining ratio

d_g = mean diameter of grain

On the stone surface which comes in contact with the work surface, the actual grain combining ratio G becomes smaller than that in the inner parts of the stone owing to the fall-off of grains. Accordingly, the value of n_a given by equation (1) can not be defined as the number of cutting points which this paper proposes to find.

In the actual finishing operation, it can be recognized that the number of cutting points n depends on the depth of cut t as shown in Fig. 1. The stone surface which
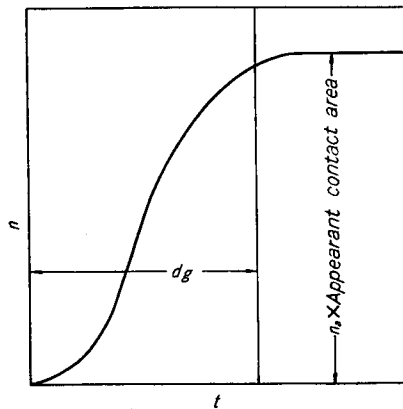

Fig. 1. Variation of number of cutting points n with cutting depth t.
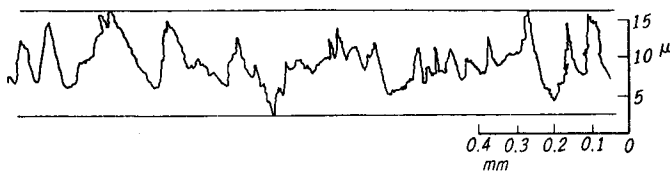

Fig. 2. Example for profile curve of abrasive stone surface using in superfinish.

comes in contact with the work in superfinishing is a rather rough surface as shown in Fig. 2. Accordingly, to investigate the number of cutting points, it is necessary to analyse the profile curve of the contact surface statisticaly.

In this paper, a statistical analysis of the contact mechanism of stone and work, an inquiry into the assumptions of this analysis, and the number of cutting points for representative conditions in using fine-grain abrosive stone are described. The validity of the theory is checked by the following method.

The theoretical mean cutting depth of abrasive grains $(t_m)_{th}$ is defined as half of the maximum depth of cut T which can be obtained from the theoretical analysis of the contact mechanism, and the value of T is calculated with the roughness of the stone surface H in actual finishing operations. The experimental mean cutting depth of abrasive grains $(t_m)_{ex}$is defined from the actual cutting depth per unit time C_t, while the value of $(t_m)_{ex}$ is found from the number of cutting points n depending on the roughness of the stone surface H. Tnan comparing the value of $(t_m)_{th}$ with the value of $(t_m)_{ex}$, the validity of the theory may be investigated.

Part I   The Theoretical Analysis for the Number of Cutting Points on the Contact Surfaace of Stone.

1.   Contact Mechanism of Stone and Work

In order to derive theoretical equations for the number of contact points and the depth of indentation with regard to a state where two nominally flat surfaces having a degree of roughness are pressed together under an applied load, the following assumptions were made:

(1)   The distribution curves of the roughness on the stone and the work obtained from the profile curve of the surface as shown in Fig. 3 have normal distributions.
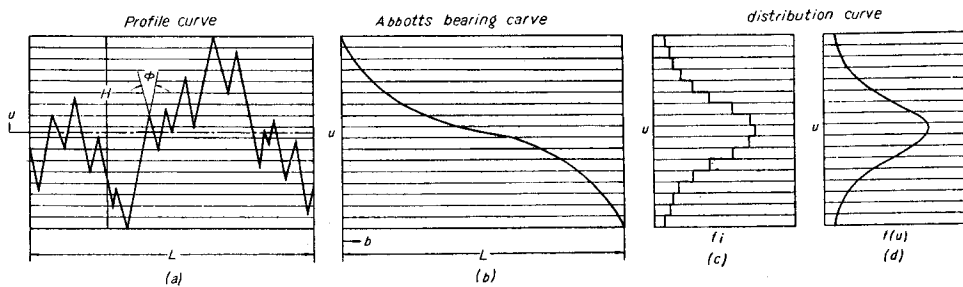

Fig. 3.   Method of drawing distribution curve from profile curve.

(2)   The profile curve of the stone surface has a curve as shown in Fig. 4 modally, i.e. the surface contains a large number of conical asperities having the equal slope angle Ψ, and the asperities are evenly distributed
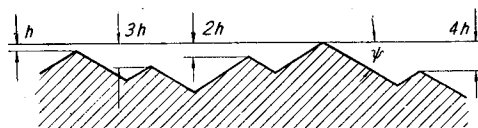

Fig. 4.   Model of profile curve on the contact surface of stone.

in the direction of the indentation ; or, stated in another way, there is one asperity at each of the h, and the waviness of the surface is disregarded.

(3) The deformation occurring in the neighbourhood of the contact point is the plastic deformation of the metal surface.

(4) The roughness of the work surface in the finishing operation using the fine-grain abrasive stone is so small compared with the roughness of the stone surface (the roughness of the work surface is $1/20 \sim 1/40$ times that of stone surface) that the work surface may be considered as an ideal flat surface in this case.

(5) The roughness of the stone surface does not change with the measuring direction of roughness, therefore, the asperity of the stone surface may be taken as the conical form.

(i) **The Number of Asperities into Contact n and the Maximum Dept of Indentation T**
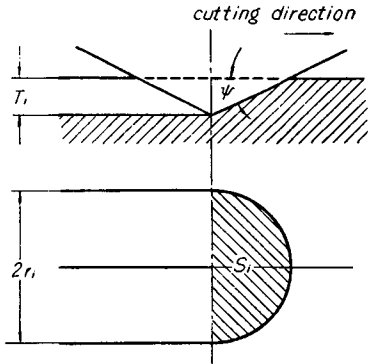

Fig. 5. Cutting model of asperity.

Assuming the plastic deformation of the metal occurring at the contact, the flow pressure p_m should be constant under any load[2]. Then, the total contact area A which was projected in the direction of the contact plane is found to be

$$A = W/p_m \qquad (2)$$

where

$$W = \text{contact load}$$

As shown in Fig. 5, it is clear that the projected contact area of one asperity S_i is given by the area of the semi-circle, that is found to be

$$S_i = \frac{\pi}{2} r_i^2 = \frac{\pi}{2} (T_i \cot \Psi)^2 \qquad (3)$$

while from assumption (2)

$$T_i = ih \qquad (4)$$

where $i = 0, 1, 2, 3, \cdots , (n-1)$
and

$$A = \sum_{i=0}^{n-1} S_i \qquad (5)$$

From equations (2), (3), (4), and (5)

$$W = p_m A = p_m \sum_{i=0}^{n-1} S_i \cong \frac{\pi}{2} p_m h^2 \cot^2 \Psi \frac{n^3}{3} \qquad (6)$$

and therefore

$$n = \left(\frac{6W}{\pi p_m h^2 \cot^2 \Psi}\right)^{1/3} \tag{7}$$

Then, if M is defined as the number of asperities into contact resulting from the indentation of unit distance, in other words, M is the number of asperities per unit depth.

$$M = 1/h \tag{8}$$

$$n = \left(\frac{6M^2 \tan^2 \Psi}{\pi p_m}\right)^{1/3} W^{1/3} \tag{9}$$

And the maximum depth of indentation T is given by

$$T = nh = \frac{n}{M} = \left(\frac{6 \tan^2 \Psi}{\pi p_m M}\right)^{1/3} W^{1/3} \tag{10}$$

Among the variables M, p_m, W and Ψ which are contained in equations (9) and (10), the contact load W and the flow pressure p_m are known values. Therefore we may investigate the number of asperities per unit depth M and the slope angle of conical asperitiy Ψ.

(ii)   The Number of Asperities into Contact Resulting from the Indentation of Unit Distance M

When the distribution curve that is obtained from the profile curve of the stone surface has a normal distribution, as shown in Fig. 3, the probability density of surface units distribution $f(u)$ is given by

$$f(u) = \frac{1}{\sqrt{2\pi}\,\sigma} e^{-1/2(u/\sigma)^2} \tag{11}$$

where

$u =$ deviation from the median line of the profile curve

$\sigma =$ standard deviation

If N is the total number of surface units contained within the measured length L, and $\varepsilon\sigma$ is the projection width which can be comprised in one surface unit, the number of intersections of the profile curve on the parallel line which has u distance from the median line of profile curve will be $Nf(u)\varepsilon\sigma$. And so the number of asperities crossed by this parallel line I is given by

$$I = \frac{1}{2} Nf(u)\,\varepsilon\sigma$$

and where $\qquad\qquad N\varepsilon\sigma = L \tan \Psi$

therefore $\qquad\qquad I = \frac{1}{2} Lf(u) \tan \Psi \tag{12}$

When the ideal flat surface moves towards this model surfrce, the contact is considered to begin at the distance of $u_0 = l\sigma$ from the median line of the profile

curve and the value of l may be determined depending upon the value of the total number of surface units contained within the measured length L. From the table of statistics, the relation between l and N is made as shown in Fig. 6. Then the value of N is found to be
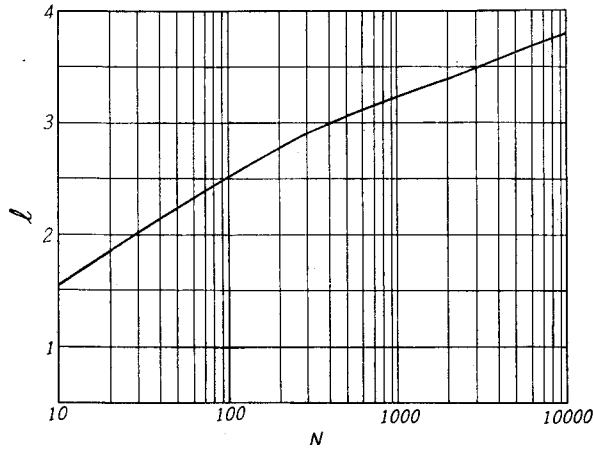

Fig. 6. Variation of l with total number of surface units N contained within the measured length L.

$$N = 2L \tan \Psi f(0) = 0.7978 \frac{L}{\sigma} \tan \Psi \qquad (13)$$

Considering the profile curve of a stone surface, it is very troublesome to calculate the value of σ for the individual profile curve of a stone surface. However, if the maximum height of asperities H, which means the distance from peak to valley measured on the profile curve of the stone surface, is equal to $j\sigma$, that is

$$H = j\sigma \qquad (14)$$

where, j depends upon the measured length L used for measuring H.

But it has been well known that j has a constant value for any profile curve of a finished metal surface notwithstanding the magnitude of H, and j is given for most cases as

$$j = 5.0 \qquad (15)$$

Considering the contact between the ideal flat surface having the apparent contact area $L_x L_y$ and the stone surface having a degree of roughness, the number of contact asperities at the begining point of contact where $u = u_0$ is found to be

$$\left\{ \frac{1}{2} L_x \tan \Psi f(u_0) \right\} \left\{ \frac{1}{2} L_y \tan \Psi f(u_0) \right\} \qquad (\text{a})$$

And the number of contact asperities indenting into a unit depth from the begining point is found to be

$$\left\{\frac{1}{2}L_x \tan \Psi f(u_0-1)\right\}\left\{\frac{1}{2}L_y \tan \Psi f(u_0-1)\right\} \qquad (b)$$

and therefore the number of asperities per unit depth M is given by

$$M = (b) - (a) = \frac{1}{8\pi}\frac{L_x L_y}{\sigma^2}\tan^2 \Psi \{e^{-(1-1/\sigma)^2}-e^{-l^2}\}$$

Then

$$M = K(e^{2Z}-1) \qquad (16)$$

where

$$K = \frac{j^2 e^{-l^2}}{8\pi}\frac{L_x L_y}{H^2}\tan^2 \Psi$$

$$Z = \frac{jl}{H} - \frac{j^2}{2H^2}$$

However, for inducing theoretical equations of n and T we have assumed that the asperities are evenly distributed and that there is one asperity at each depth of h. Then, in order to minimize the calculation error due to this assumption, the maximum depth of indentation T which is found at the contact conditions coming into question in this case must be chosen for the unit length using to the calculation of M. Further, in equations (9) and (10), T must be taken as the unit of length for the quantity contained within the dimension of length.

In order to carry out easily, the calculation mentioned above the following equation for Z' is used as a substitute for the Z of equation (16) for a group of T which measured in the common unit of length.

$$Z' = \frac{jl}{H}T - \frac{j^2}{2H^2}T^2 \qquad (17)$$

And the value of M is obtained from this equation. If equation (9) is solved for W by way of $n=M$, we obtain

$$W = \frac{\pi p_m n}{6\tan^2 \Psi}T^2 \qquad (18)$$

From this W, values of n and T with regard to a certain value of W can be obtained graphically. In this case, the common unit of length can be used to measure the value of H, p_m and T. Some representative results for the calculation of T and n are shown in Fig. 7 and Fig. 8.

(iii) The Slope Angle of Asperity Ψ

From the slope angle of the profile curve measured at the contact surface of the stone considered along with the magnification of a profile measuring machine, it is possible to find the slope angle of asperity. The slope angle of asperity Ψ thus measured in the neighbourhood of the median line of the profile curve where the curve is comparatively straight is $19° \sim 25°$. However as for contact mechanism, the value of Ψ required is the value at the extremity of the asperity where the contact actually occurs. Therefore, the value of Ψ used in this calculation is obtained by the following method.
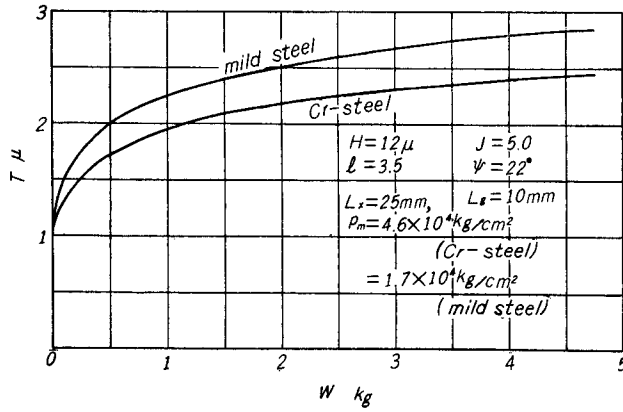
Fig. 7. Variation of maximum depth of cut T with contact load W.
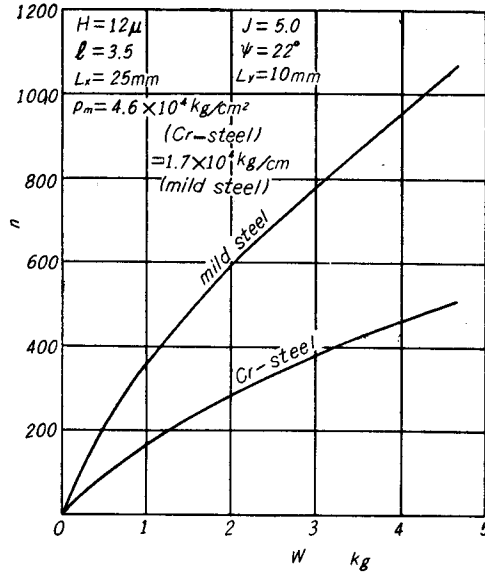
Fig. 8. Variation of number of cutting points n with contact load W.

We consider the case where an ideal flat surface is pressed against the stone surface to a depth T. When it is assumed that the grains distributed on the stone surface have a spherical form with a mean diameter d_g, the total true contact area A_s is obtained from the following equation.

$$A_s = \frac{\pi}{2} \sum_{i=0}^{n-1} \frac{1}{n-1} T\left(d_g - \frac{1}{n-1} T\right)$$

$$\simeq \frac{\pi}{2} nT\left(\frac{d_g}{2} - \frac{T}{3}\right) \tag{19}$$

Fig. 9. Variation of slope angle of
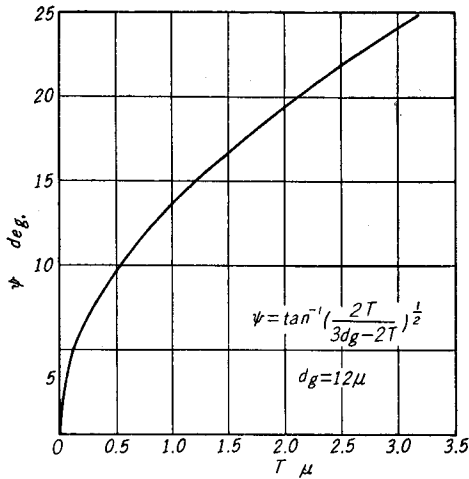   asperity Ψ with maximum
         depth of cut T.

And when it is assumed that the grains distributed on the stone surface have a conical form and a slope angle of Ψ, the total true contact area A_c is calculated from the following equation.

$$A_c = \frac{\pi}{2} \sum_{i=0}^{n-1} \left(\frac{1}{n-1} \frac{T}{\tan \Psi} \right)^2$$

$$\cong \frac{\pi}{6} \frac{nT^2}{\tan^2 \Psi} \qquad (20)$$

Then the value of Ψ is chosen so that the value of A_s is equal to the value of A_c. From equations (19) and (20),

$$\Psi = \tan^{-1} \left(\frac{2T}{3d_g - 2T} \right)^{1/2} \quad (21)$$

As to the mean diameter of grain $d_g = 12\mu$, the relation between Ψ and T is shown in Fig. 9.

2. The Investigation of the Assumations about the Contact Mebhanism and the Relation between the Number of Asperities into Contact and the Number of Cutting Points on the Contact Surface of the Stone.

(i) The Investigation of Assumtions

Among the five assumptions mentioned above, the first one must be investigated. In general, it has been recognized that the distribution curve of a profile curve of a metal finished surface has a normal distribution approximately. But in the stone there are grains, bond and pores. The existence of pore parts is especially characteristic of the stone surface. It con be seen that the existence of pore parts on the stone surface will result in the expansion of the valley parts of the profile curve. The actual profile curve of a stone surface measured during the superfinishing operation is investigated in the same way as shown in Fig. 3.

An example of this type of investigation is as follow :

The working conditions of superfinish ;

Abrasive stone

Size : $10 \times 15 \times 30$ mm, abrasiue grain : Aluminum oxide, grit : 600 mesh, bond : vitrified,

grade : Rockwell H hardness 60.

Work material : Cr-steel (C 0.94%, Cr 1.61%)

Motional conditions

Work speed : 11.5 m/min, frequency of stone :

1200 cycle/min, amplitude of stone : 3 mm.

Stone pressure : 2.5 kg/cm²

In this case, the roughness of the stone surface H is obtained as follow :

$$H = 11.8\mu$$

And the calculated results of Abbott's bearing curve and the distribution curve obtained from H for the measured length $L = 3$ mm are shown in Fig. 10. In the figure, f_i is obtained from Abbott's bearing curve, and $f(u)$ is calculated from the standard deviation of this profile curve. From these results, it was possible to
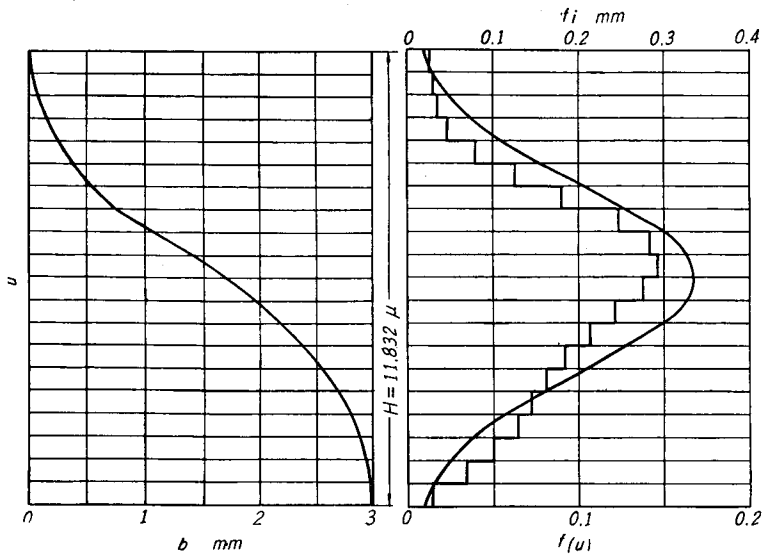
Fig. 10. Probability density of surface units distribution data
obtained from stone surface using in superfinish.

assume a normal distribution for the profile curve obtained from the stone surface because we could not find any difference in f_i between the stone surface and the finished metal surface.

Moreover, we obtained in this case,

$$\sigma = 2.39$$

and therfore, from equation (14)

$$j = 4.95$$

Hence, as to the value of j on the stone surface, it follows that j is 5 independent of the magnitude of H, as in the case of the finished metal surface as shown in equation (15). The investigations of the other assumptions are abbreviated.

(ii) **The Relation between the Number of Asperities and the Number of
Cutting Points**

The value of n calculated from equation (9) is the number of conical asperities
in contact with the ideal flat surface. As for the abrasive stone, the extremity part
of an asperity along the contact surface is formed with one grain but the base of
the asperity is formed from more than two grains. Then, depending upon the value
of the maximum depth of indentation T, there exists a critical value where it becomes
impossible use equation (9) for the number of cutting points on the stone surface.

That critical value for equation (9) is determined by considering the asperity
which has the maximum depth of indentation. If the maximum contact area of one
asperity $S_{\max}$ calculated from equation (3) is smaller than half the sectional area of
one grain, that is,

$$S_{\max} = \frac{\pi}{2}(T \cot \Psi)^2 < \frac{\pi}{8}d_g^2 \tag{22}$$

Then the number of cutting points on the contact stone surface is found to be the
number of contact asperities calculated from equation (9), since it is impossible for
more than 2 grains to exist in the sectional area of one grain. Using equations (21)
and (22), the critical value of indentation depth $T_{\max}$ is found to be

$$T_{\max} = \frac{3-\sqrt{5}}{4}d_g \simeq 0.2\,d_g \tag{23}$$

3. The Relation between the Number of Cutting Points
and the Roughness or the Size of Contact Stone Surface

Depending upon the working condition, the characteristics of contact stone sur-
faces are classified into three ranges as reported before[3], that is, in the first
range called "cutting" grains fall-off and in the second range called "semi-cutting"
grains occur the cleavage and in the last range called "mirror-finishing" the contact
stone surface is loaded all over. Accordingly, the roughness of the contact stone
surface H is considerably changed by the working conditions. In order to show the
relation between H and n or T diagrammaticaly, the following equations are derived
from equations (9), (10), (16), (17) and (21).

$$n = K'(e^{2z'}-1)\,\varphi(T) \tag{24}$$

$$W = \frac{\pi p_m n}{6\varphi(T)}\,T^2 \tag{25}$$

where
$$K' = \frac{j^2 e^{-l^2}}{8\pi}\frac{L_x L_y}{H^2}\,, \qquad \varphi(T) = \frac{2T}{3d_g-2T}$$

$$Z' = \frac{jl}{H}T - \frac{j^2}{2H^2}T^2$$

And the common unit of length can be used in these equations.

For this calculation, the roughness of the contact stone surface H is chosen in the range of $5\sim20\mu$ which can be measured in the actual finishing operation using the fine-grain abrasive stone. Further, when the material of work is Cr-steel, that is, $p_m=4.6\times10^4$ kg/cm^2 and the apparent contact area of the stone surface $L_xL_y=10\times10$ mm and the mean diameter of grain is $d_g=12\mu$, then diagrams of $H-n$, $H-T$, and $n-T$ are obtained as shown in Fig. 11~Fig. 13. From Fig. 11, it may be clear that the curve of the number of cutting points n decreases with increasing surface roughness of stone H, the rate of decrease continually diminishing. And the values of H and T are in proportion approximately as shown in Fig. 12. The relation between n and T can be written as follows in this case.

$$T = k_1 \ln n + k_2 \tag{26}$$

where k_1, k_2 = constants

The relation between the number of cutting points and the size of contact stone surface is shown in Fig. 14. In this figure, p means the stone pressure. When the stone pressure p is constant, the number of cutting points n is directly proportional to the length of contact stone surface L_y. But when the contact load W is constant, the number of cutting points n does not change with a change in the length of the contact stone surface L_y as shown in Fig. 15.

When the mean diameter of grain $d_g=12\mu$, the number of grains per sq. cm which is defined from equation (1) is found to be

$$n_a = \frac{6}{\pi}\frac{0.45}{12^2}\times10^8 \cong 6\times10^5 \tag{27}$$
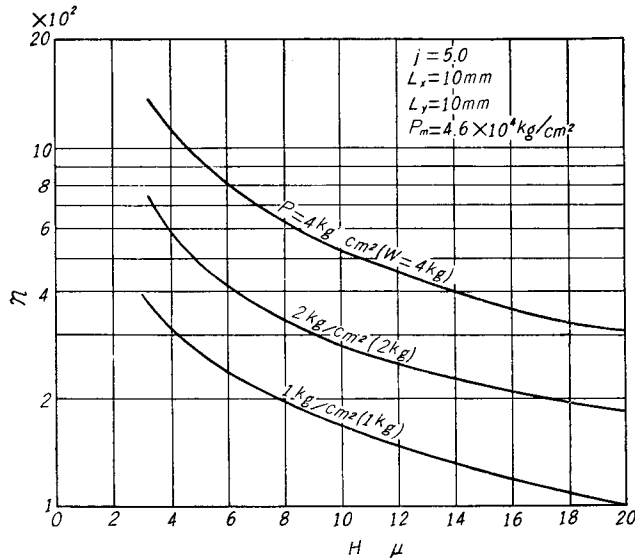
Fig. 11. Variation of number of cutting points n
with roughness of stone surface H.

Comparing the number of cutting points n obtained from the theoretical analysis as shown in Fig. 10 with the number of grains n_a which is obtained from equation (27), it may be found that n_a is $10^2 \sim 10^3$ times n.
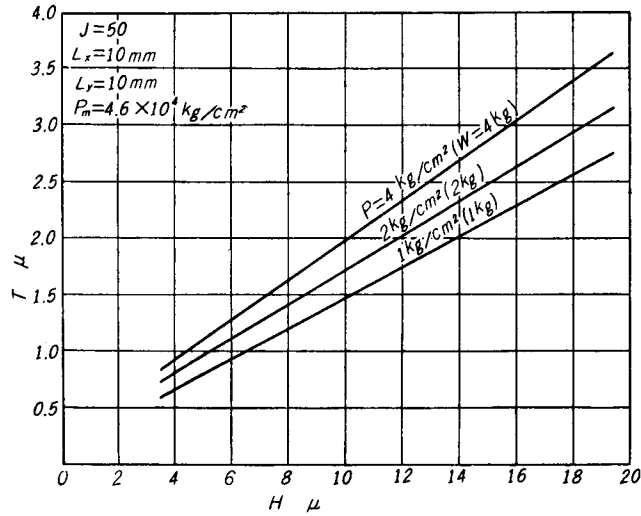
Fig. 12. Variation of maximum cutting depth T with roughness of stone surface H.

Fig. 13. Variation of number of cutting points n with maximum cutting depth T.

Fig. 14. Variation of number of cutting points n with roughness
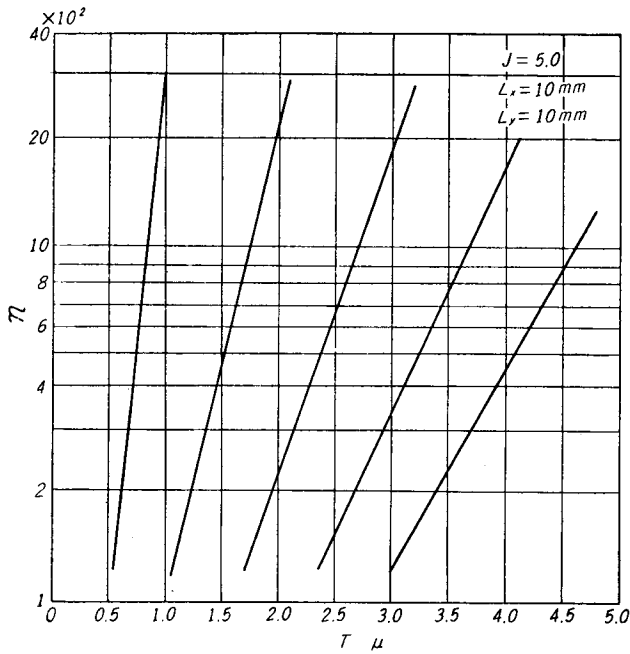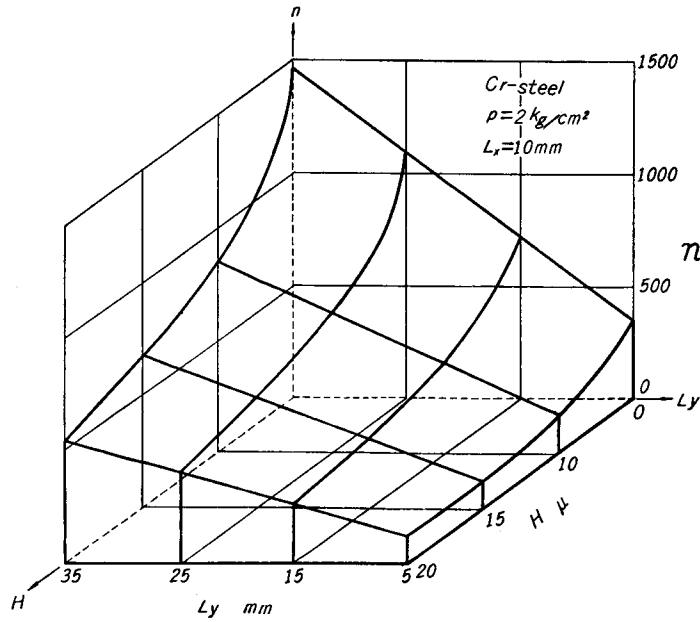of stone surface H and stone length L_y obtained under
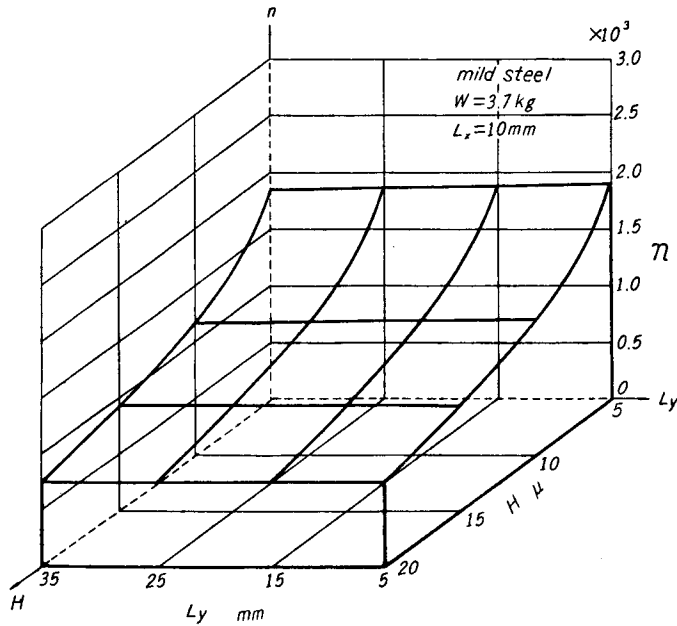the constant stone pressure p.

Fig. 15. Variation of number of cutting points n with roughness
of stone surface H and stone length L_y obtained under
the constant contact load W.

Part II. The Experimental Investigation of the Number of
Cutting Points on the Contact Surface of Stone

1. Mean Cutting Depth of Abrasive Grains

The theoretical mean cutting depth of abrasive grains which can be found with the theoretical analysis of the contact mechanism is as follows:

$$(t_m)_{th} = \frac{1}{2} \left(\frac{6 \tan^2 \Psi}{\pi p_m M} \right)^{1/3} W^{1/3} \tag{28}$$

While, the stock removal per unit time vol_w is the product of the apparent contact area A_w and the cutting depth per until time C_t.

$$vol_w = A_w C_t \tag{29}$$

When S_c is the mean cutting sectional area of grains and $\bar{v}$ is the mean relative cutting speed of work and stone,

$$vol_w = n\bar{v} S_c \tag{30}$$

where, n = number of cutting points on the contact surface of stone
and

$$S_c = (t_m)_{ex}^2 / \tan \Psi \tag{31}$$

where, $(t_m)_{ex}$ = experimental mean cutting depth of abrasive grains,
thus eliminating vol_w,

$$(t_m)_{ex} = \left(\frac{A_w C_t}{\bar{v} n} \tan \Psi \right)^{1/2} \tag{32}$$

2. Selection of Experimental Conditions and Method of Experiment

The experiment is carried out with a superfinishing operation which is a representative finishing operation using the fine-grain abrasive stone. In a superfinishing operation, there are many factors which influence the cutting performance of abrasive stone. However, as reported already[3], the characteristics of superfinish are classified into three type, i.e., "cutting", "semi-cutting" and "mirror-finishing", depending upon the condition of the contact surface of work and stone. We call this fact as the "critical phenomenon" here after, and the cutting performance of abrasive stone can be controlled by this phenomenon. Therefore, when experiments containing the above three types are carried out for each abrasive stone, the validity of the contact theory may be clarified.

As to the work material, Cr-steel which has a large flow pressure and is used widely in superfinishing operations was chosec, and the flow pressure p_m is taken as

$$p_m = 4.6 \times 10^4 \, \text{kg/cm}^2$$

In order to find the effect of the hardness of the work material, mild steel which has a lower hardness and a lower flow pressure $p_m = 1.7 \times 10^4 \, \text{kg/cm}^2$ was used.

The abrasive stones used in this experiment have the following designations :—

abrasive grain : Aluminum oxide, grit : 600 mesh, bond : vitrified. The bond combining ratio B, bond hardness R_H, porosity P, specific weight ρ and grain combining ratio G are tabulated in Table 1. The size of the contact surface of abrasive stone is 25 ×10 mm, and the diameter of the grains in these stones are distributed over the range $5 \sim 28 \mu$ and the mean diameter of the grains d_g is 12μ.

Table 1. Summary of Properties of Various Stone.

$B \%$	R_H	$P \%$	ρ	$G \%$
8	29	48.5	1.89	45.3
9	33	48.2	1.89	45.1
11	46	48.0	1.89	44.1
13	53	47.8	1.88	42.8
14	65	47.2	1.91	43.0
15	70	46.2	1.93	43.0
16	78	45.5	1.94	43.3

In order to carry out the experiment containing the critical points of cutting and mirror-finishing, five to eight kinds of cutting direction angles Θ are chosen for each abrasive stone shown in Table 1 with constant values of stone pressure p and work speed v_w. Furthermore, the frequency of stone f which is so chosen so as to obtain cutting direction angles corresponding to the critical values of cutting and mirror-finishing is made as equal as possible for all abrasive stones in Table 1. In this experiment, the amplitude of stone a is 3 mm, and the cutting fluid is a mixture of kerosene (80%) and machine oil (20%).

3. Experimental Results

The results for the cutting depth per unit time C_t and the roughness of cantact surface of stone H with regard to the experiment containing the critical points of cutting and mirror-finishing under the constant stone pressure $p = 2.66 \, \text{kg/cm}^2$ are shown in Tables 2 and 3. In these tables, the main working conditions such as the bond hardness of stone R_H, working time m, frequency of stone f, mean cutting speed $\bar{v}$ and cutting direction angle Θ are shown also. In the column of finishing characteristics, $\bigcirc$, $\circlefthalfblack$ and $\bullet$ show "cutting", "semi-cutting" and "mirror-finishing" respectively. Table 2 shows the results for Cr-steel and Table 3 for mild steel.

The relation between the cutting direction angle Θ and the cutting depth per unit time C_t for C_r-steel is shown is Fig. 16. The cutting depth per unit time C_t has a very small value in the range of "mirror-finishing", and the maximum cutting depth is found in the neighbourhood of the critical curve of "cutting" in the range of "semi-cutting", and C_t is seen to rise with a decrease in the bond hardness of the stone. But the stone wear increases with decreasing bond hardness of the stone,

Table 2. Summary of Working Conditions and Measurements for Cr-steel.

B (R_H)	m min	f $\sim$/min	$\bar{v}$ m/min	θ deg.	C_t μ/min	H μ	Finishing Characteristics
16 (79)	2.5	2 700	18.0	75.2	4.00	14.2	○
	3.0	2 000	14.3	70.4	3.20	14.0	○
	4.0	1 480	11.5	64.3	3.60	13.3	◑
	4.0	1 060	9.6	56.0	2.50	12.5	◑
	5.0	910	9.0	51.9	0.54	7.6	●
	5.0	780	8.6	47.6	0.42	7.1	●
	5.0	630	8.1	41.5	0.20	6.8	●
14 (69)	2.0	2 660	24.3	54.9	7.20	16.1	○
	2.0	2 160	22.5	49.2	6.60	15.0	○
	2.0	1 900	21.5	45.5	8.05	14.0	◑
	2.5	1 540	20.1	39.5	8.04	12.5	◑
	2.5	1 260	19.3	34.0	7.12	10.5	◑
	2.5	1 050	18.8	29.4	1.52	9.3	●
	2.5	900	18.4	25.8	0.92	8.6	●
	3.0	690	18.0	20.3	0.47	8.2	●
13 (54)	1.5	2 600	33.9	39.9	8.13	18.2	○
	1.5	2 180	32.6	35.0	8.07	18.1	○
	1.5	1 750	31.4	29.3	8.60	17.6	◑
	1.5	1 480	30.7	25.4	8.40	17.2	◑
	1.5	1 150	30.1	20.3	8.33	15.0	◑
	1.5	830	29.8	14.9	2.00	14.3	●

Table 3. Summary of Working Conditions and Measurements for Mild Steel.

| B (R_H)	m min	f $\sim$/min	$\bar{v}$ m/min	θ deg.	C_t μ/min	H μ	Finishing Characteristics
16 (79)	3.0	1 960	12.6	71.5	5.3	16.5	○
	4.0	1 350	10.9	63.4	4.3	15.5	○
	4.0	1 180	10.1	60.2	4.3	14.3	○
	5.0	800	8.5	49.8	3.8	13.6	◑
	5.0	650	8.0	43.9	3.2	9.8	◑
	5.0	480	7.6	35.4	0.5	7.5	●
14 (69)	2.0	2 250	22.4	54.0	10.0	17.5	○
	2.0	2 000	21.2	50.8	9.8	16.2	○
	2.5	1 500	19.6	42.6	9.1	14.8	◑
	2.5	1 250	18.9	37.4	8.4	13.3	◑
	2.5	970	18.4	30.7	3.0	10.6	●
13 (54)	1.5	2 240	32.4	37.6	15.5	19.5	○
	1.5	1 450	30.5	26.5	15.2	19.2	◑
	1.5	960	29.8	18.3	12.0	16.3	◑
	1.5	550	29.5	10.7	11.8	15.5	◑
	1.5	360	29.2	7.1	8.7	14.6	●
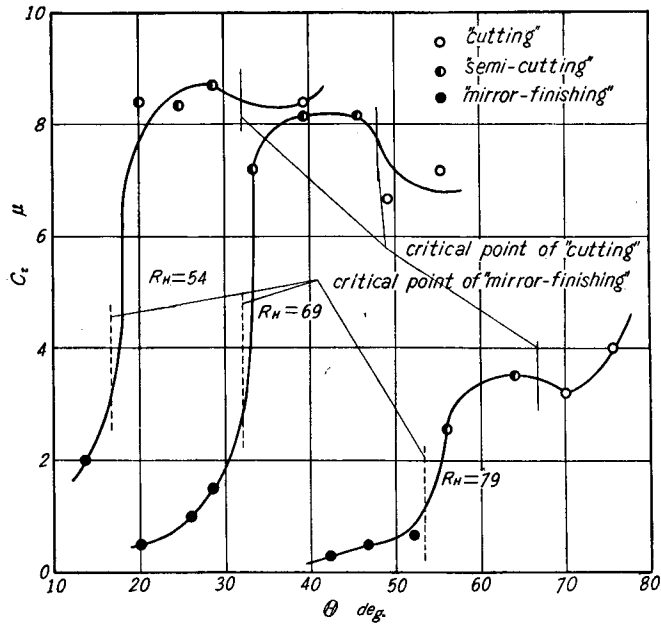
Fig. 16. Variation of cutting depth C_t with cutting direction
angle θ about various bond hardness of stones.

As shown in Fig. 17, the roughness of the stone surface H increases linearly
with increasing cutting direction angle θ in the ranges of "cutting" and "semi-
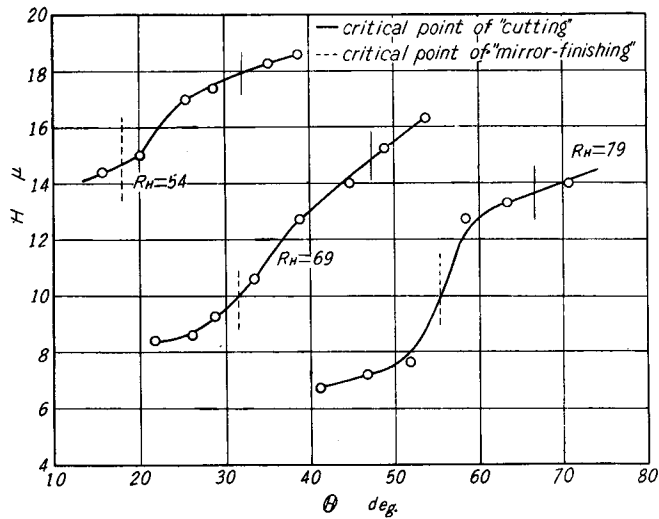cutting", and the increasing tendency of H curves in the ranges of "semi-cutting"

Fig. 17. Variation of roughness of stone surface H with cutting
direction angle θ about various bond hardness of stones.

and "mirror-finishing" are smaller than that of the C_t curve which is shown in Fig. 16. Moreover, H increases with decreasing bond hardness of stone R_H. But H shows comparatively little change with work materials.

The data of Table 4 show the results for tests with varying stone pressure p. It is evident that the cutting depth C_t varies extremely with a variation in stone pressure, and that when the stone pressure varied over a wide range, the stone pressure had comparatively little influence upon the roughness of the stone surface H.

Table 4. Effect of Stone Pressure on Cutting Depth and Roughness of Stone Surface.

p kg/cm²	C_t μ/min	H μ
3.36	12.4	18.0
2.66	8.6	17.6
1.96	2.0	16.5

4. Calculation of the Mean Cutting Depth of Abrasive Grains

Corresponding to the working conditions shown in Tables 2 to 4, the relations between H and n or H and $(t_m)_{th}$ which is obtained from the theoretical investigation of the contact mechanism are shown in Figs. 18 and 19. The values of n and $(t_m)_{th}$ corresponding to the values of roughness of the stone surface H measured in these tests are found from Figs. 18 and 19, and the results are shown in Tables 5 to 7. Tables 5 to 7 correspond to Tables 2 to 4 respectively.
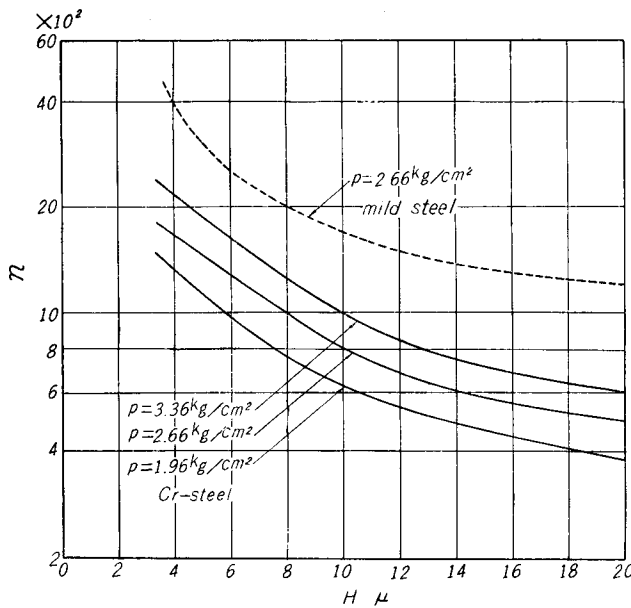

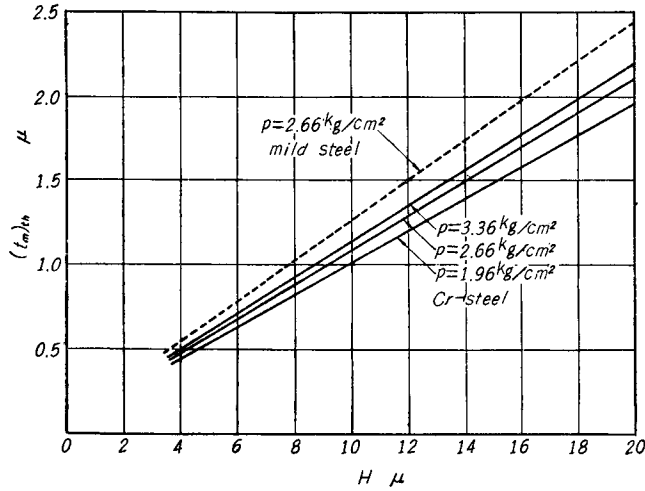Fig. 18. Variation os number of cutting points n with roughness of stone surface H.

Fig. 19.   Variation of theoretical mean cutting depth $(t_m)_{th}$
with roughness of stone surface H.

Table 5.   Data obtained under the Conditions of Table 2.

B (R_H)	Θ deg.	Finishing Characteristics	n	$(t_m)_{th}$ μ	Ψ deg.	$(t_m)_{ex}$ μ	$\dfrac{(t_m)_{th}}{(t_m)_{ex}}$
16 (79)	75.2	○	615	1.51	12.5	0.44	3.4
	70.4	○	620	1.49	12.4	0.43	3.5
	64.3	◐	640	1.42	13.8	0.53	2.7
	56.0	◐	675	1.34	12.7	0.45	3.0
	51.9	●	1 010	0.84	6.5	0.13	6.5
	47.6	●	1 070	0.80	5.9	0.11	7.3
	41.5	●	1 110	0.77	4.2	0.06	12.8
14 (69)	54.9	○	560	1.70	14.3	0.57	3.0
	49.2	○	590	1.59	14.5	0.54	2.9
	45.5	◐	620	1.49	15.0	0.62	2.4
	39.5	◐	675	1.34	14.9	0.61	2.2
	34.0	◐	765	1.14	13.8	0.53	2.2
	29.4	●	860	1.02	7.8	0.18	5.7
	25.8	●	920	0.94	6.2	0.12	7.8
	20.3	●	955	0.91	5.0	0.08	11.4
13 (54)	39.9	○	525	1.91	13.5	0.51	3.7
	35.0	○	530	1.90	13.7	0.52	3.6
	29.3	◐	540	1.85	14.1	0.55	3.4
	25.4	◐	545	1.80	14.0	0.54	3.3
	20.3	◐	590	1.59	13.7	0.52	3.1
	14.9	●	610	1.52	8.2	0.20	7.6

Table 6. Data obtained under the Conditions of Table 3.

B (R_H)	θ deg.	Finishing Characteristics	n	$(t_m)_{th}$ μ	Ψ deg.	$(t_m)_{ex}$ μ	$\dfrac{(t_m)_{th}}{(t_m)_{ex}}$
16 (79)	71.5	○	1 300	2.04	12.1	0.41	5.0
	63.4	○	1 320	1.91	11.8	0.39	4.9
	60.2	○	1 390	1.78	11.8	0.39	4.5
	49.8	◐	1 420	1.69	11.9	0.40	4.2
	43.9	◐	1 770	1.24	10.6	0.32	3.9
	35.4	●	2 180	0.96	5.0	0.08	12.0
14 (69)	54.0	○	1 270	2.16	12.4	0.43	5.0
	50.8	○	1 310	2.00	12.4	0.43	4.6
	42.6	◐	1 370	1.84	12.2	0.42	4.4
	37.4	◐	1 430	1.68	11.9	0.40	4.2
	30.7	●	1 660	1.33	7.8	0.18	7.4
13 (54)	37.6	○	1 200	2.39	12.9	0.47	5.1
	26.5	◐	1 210	2.36	13.1	0.48	4.9
	18.3	◐	1 310	2.01	11.9	0.40	5.0
	10.7	◐	1 320	1.91	11.8	0.39	4.9
	7.1	●	1 380	1.81	10.4	0.31	5.8

Table 7. Data obtained under the Conditions of Table 4.

p kg/cm²	n	$(t_m)_{th}$ μ	Ψ deg.	$(t_m)_{ex}$ μ	$\dfrac{(t_m)_{th}}{(t_m)_{ex}}$
3.36	640	1.97	15.1	0.63	3.2
2.66	540	1.85	14.1	0.55	3.3
1.96	430	1.64	9.9	0.28	5.8

As shown in Table 5, it is clear that the number of cutting points on the contact surface of stone which has a contact area A_w of 2.5 cm² are 500~1100. On the other hand, the number of grain (n) which intersect the optional plane having the area A_0 of 2.5 cm² within the stone is calculated as follows

$$(n) = \frac{6}{\pi}\frac{G}{d_g^2}A_0 = 1.43 \times 10^6$$

where $G = 0.43$ (see Table 1)

$d_g = 12\mu$ mean diameter of grains

Comparing the values of (n) with n, (n) is 1000–3000 times n.

Then the experimental mean cutting depth of abrasive grains $(t_m)_{ex}$ is calculated from equation (32) using the cutting depth C_t shown in Tables 2 to 4. But $\tan\Psi$ in the equation is a function of t_m as follows

$$\tan\Psi = \left(\frac{4t_m}{3d_g - 4t_m}\right)^{1/2}$$

Accordingly, the calculation of $(t_m)_{ex}$ is carried out by means of the following method, that is, from equation (32)

$$(t_m)_{ex} = f(C_t)(\tan \Psi)^{1/2}$$

where

$$f(C_t) = \left(\frac{A_w C_t}{\bar{v}n}\right)^{1/2}$$

Fig. 20 shows the relation between t_m and $(\tan \Psi)^{1/2}$. As to the value of $(t_m)_{ex}$ we chose the value of the horizontal coordinate t_m in Fig. 5, so that it may be equal to the product of $(\tan \Psi)^{1/2}$ and $f(C_t)$ which is calculated from C_t, $\bar{v}$ and n as shown in Tables 2 to 7. The values of $(t_m)_{ex}$ obtained in this way, Ψ and $(t_m)_{th}/(t_m)_{ex}$ are tabulated together in Tables 5 to 7.

From these Tables, it is clear that the slope angle of the conical asperity Ψ takes a value of $12°\sim14°$ in the range of "cutting". When the cutting edge on the
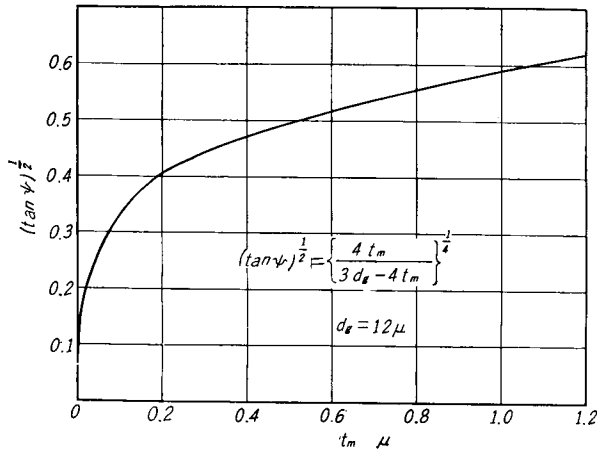

Fig. 20. Variation of $(tan\ \Psi)^{1/2}$ with mean cutting depth t_m.

stone surface has this slope angle, the profile curve of the work surface which has been finished by this stone should be about the same as the slope angle. Actually, there is comparatively good agreement between the calculated value of slope angle and that of the measurements of the profile curves in superfinished surfaces. The value of the experimental mean cutting depth of grains $(t_m)_{ex}$ has little or no change with the bond hardness of the stone, and it is $0.4\sim0.6\mu$ in the range of "cutting" and "semi-cutting", but it has a very small value and is occasionally less than 0.1μ in the range of "mirror-finishing".

5. Discussions of th Experimental Results

Comparing the theoretical value with the experimental value of the mean cutting

depth of grains by the ratio of $(t_m)_{th}$ and $(t_m)_{ex}$ as shown in Tables 5 to 7, the the-oretical value which is in closest agreement with the experimental values from these tests is 2.2 times the experimental value. Then, considering the causes which produce differences in both values of the mean cutting depth of grains, it is evident that the following factors cause differences to arise between the theoretical cutting state in which the work is assumed to be cut by conical asperities with plastic deformation and actual superfinishing state:

(1)   In deriving the equation for $(t_m)_{ex}$, we assumed that the stock removal per unit time vol_w is given by $n\bar{v}S_c$, but the cutting edge of the grain can not cut all parts of the cutting sectional area S_c, and a considerable part of S_c will
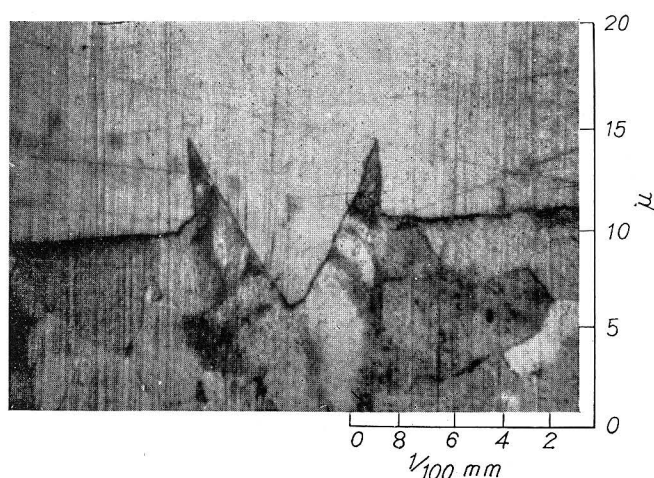

Fig. 21.   Profile of seratch showing swelling-up.

remain on the work surface as a swelled up portion as shown in Fig. 21. Accordingly, $(t_m)_{ex}$ calculated from equation (32) using the value of C_t which may be obtained from the actual removed volume is clearly smaller than $(t_m)_{th}$.
(2)   There is the case where the cutting depth of the grain diminishes due to grain cleavage or the fall-off. Therefore, the cutting depth per unit time C_t becomes smaller than we had assumed theoretically, and $(t_m)_{ex}$ diminishes.
(3)   From the actual contact mechanism of stone and work, it is well to consider that the axis of the conical cutting asperity can be taken to the optional direc-tions against the work surface. Hence the axes of some conical asperities do not take the perpendicular direction against the work surface. Therefore, the tendency of $(t_m)_{ex}$ to diminish becomes rather maked due to the fact that the actual true contact area of the work and the stone may have a greater value than we had assumed theoretically.

(4) The contact pressure becomes smaller than the measured value of it, due to the fact that the lubricating action of the cutting fluid poured into the contact surface of work and stone increases with the increasing smoothness of the work surface. This phenomenon also causes $(t_m)_{ex}$ to becomes smaller.

(5) It can be seen that the roughness of the stone surface H measured by the needle method is larger than that in the actual operation due to the removal of chips and grains which are stuffed in the pores of the stone surface. $(t_m)_{th}$ increases linearly with increasing H. On the other hand, n decreases with increasing H, and $(t_m)_{ex}$ increases with decreasing n. Namely, both values of $(t_m)_{th}$ and $(t_m)_{ex}$ are increased when the roughness of the stone surface H increases. However, the rate of increase of $(t_m)_{th}$ with an increment in H is larger than that of $(t_m)_{ex}$, because in equation (32) $(t_m)_{ex}$ is proportional to $n^{-1/2}$.

Among the five causes mentioned above, the first cause and the third cause are active in all ranges of finishing characteristics. Considering the relation between the other causes and the finishing characteristics, it is clear that the minimum value of $(t_m)_{th}/(t_m)_{ex}$ can be found in the range of "semi-cutting". Namely, in the range of "cutting" the influence of the second cause is large due to the fact that a large amount of cleavage and the fall-off of grains occurs in this range, and in the range of "mirror-finishing" the influences of the fourth cause and the fifth cause are large. Accordingly, the minimum value of $(t_m)_{th}/(t_m)_{ex}$ can be found in the range of "semi-cutting" where cleavage and fall-off of grains are very small and the lubricating action of the cutting fluid and the loading of the stone surface are small. Then it is well to consider that the most essential cause of the difference between $(t_m)_{th}$ and $(t_m)_{ex}$ is the swelling-up mentioned in the first cause. From the result of experimental investigation, it is clear that the volume of the swelling-up reaches a value more than 60% of the cutting volume obtained from the theoretical investigation. Considering this fact, it may be recognized that $(t_m)_{ex}$ is nearly equal to $(t_m)_{th}$ in the range of "semi-cutting".

The number of cutting points on the stone surface is investigated in accordance with the discussion of the mean cutting depth of grains mentioned above. The causes which produce differences between the number of cutting points in the actual operation and the number of cutting points obtained from the theoretical analysis are the third through the fifth of the five causes.

In the actual finishing operation the third cause and the fourth cause result in a smaller value for the number of cutting points than the theoretical value, but the fifth cause results in a larger value. However, in the range of "semi-cutting" the influence of these causes on the number of cutting points is small and $(t_m)_{th}$ is equal to $(t_m)_{ex}$. In the range of "cutting" the influence of the fourth cause is small

and the influences of the third cause and the fifth cause cancel each other. Therefore, in the ranges of "cutting" and "semi-cutting" where the cutting action is the subject of discussion, the number of cutting points on the stone surface can be obtained from the theoretical equation.

Conclusions

As a result of the theoretical analysis of the contact mechanism of stone and work, the number of cutting points and the maximum depth of cut are obtained as functions of the roughness and the asperity of the stone surface, the pressure on the stone and the hardness of the work material.

Comparing the number of grains on the contact stone surface with the number of grains in the inner part of the stone, it is found that the number of cutting points on the stone surface obtained from the theory is less than 1/100 times the number of grains which intersect the optional plane in the inner part of stone.

In order to check the validity of the equation of the number of cutting points on the stone surface, the experimental mean cutting depth $(t_m)_{ex}$ which can be obtained from the stock removal per unit time and the number of cutting points on the stone surface is compared with the theoretical mean cutting depth $(t_m)_{th}$ which can be obtained from the analysis of the contact mechanism of stone and work under the various working conditions. As a result of this investigation, the following conclusions are obtained.

The smallest difference of $(t_m)_{th}$ and $(t_m)_{ex}$ is found in the range of "semi-cutting" and the largest difference of $(t_m)_{th}$ and $(t_m)_{ex}$ is found in the range of "mirror-finishing". $(t_m)_{th}$ is larger than $(t_m)_{ex}$ in all the finishing characteristics. Considering the influence of the causes which produce the difference between $(t_m)_{th}$ and $(t_m)_{ex}$ on the number of cutting points on the stone surface, the number of cutting points on the stone surface can be obtained from the theoretidal equation in tne ranges of "cutting" and "semi-cutting" where the cutting action is the subject of discussion.

References

1) G. S. Reichenbach, J. E. Mayer, S. Kalpakcioglu and M. C. Shaw; Trans. ASME, 78 (1956).
2) D. Tabor; The Pro. of the Phy. So. 67, 249 (1954).
3) T. Sasaki and K. Okamura; THIS MEMOIRS, XVI (1954).